CHAPTER 10

Current State and Disintegration of Rock-Glacier Landforms in Tempe Terra, Mars

Abstract

The fretted terrain at the Martian dichotomy boundary exhibits a variety of creep-related morphologies generally known as lobate debris aprons and lineated valley fills. We here investigate debris aprons and adjacent terrain in the Tempe Terra/Mareotis Fossae region (270-294°E, 46-54°N) and provide observational evidence for several stages and mechanisms of debris supply at remnant massifs, i.e., rock fall and landsliding in a sequence with (cyclic) deposition and disintegration of a widespread surficial mantling deposit. The mantling deposit disintegrates by processes similar to thermokarstic degradation as indicated by heavily dissected areas and characteristic shallow and aligned circular depressions. Correlations of geomorphometric key values in a global context show that the Tempe Terra/Mareotis Fossae debris aprons are comparable to other characteristic locations of debris aprons on Mars. These key values do not show any significant dependencies to geographic locations (e.g., latitudes) suggesting that an equilibrium state of debris advance and deformation has been reached globally before disintegration processes initiated.
Comparisons of theoretically derived cross-section profiles to topographic measurements across lineated-valley fill units as well as lobate debris aprons provide additional clues that such creep-related landforms are currently degrading. Such processes are probably active today as geomorphologic features appear pristine and crater-size frequency measurements yield ages in the range of 50-100 Ma only and would support the idea of climatically driven degradation at Martian mid-latitudes in geologically recent times.

10.1. Introduction and Background

A variety of landforms indicates the possible existence of past or present ice in the near subsurface of Mars (e.g., *Sharp*, 1973; *Carr and Schaber*, 1977; *Rossbacher and Judson*, 1981; *Lucchitta*, 1981). Among the most prominent ice-related features are lobate debris aprons. They have been interpreted to be a mixture of rock particles and ice (*Squyres*, 1978, 1979, e.g.,) analogous to terrestrial rock glaciers, i.e., debris transport systems comprising a mixture of rock fragments and segregational and/or interstitial ice (e.g., *Barsch*, 1996)). The analogy between terrestrial rock glaciers and Martian lobate debris aprons is mainly based on (a) the lobate shape of debris aprons in plan view, (b) the cross-sectional convex-upward profile indicating the style of deformation, [c] characteristic sets of ridges and furrows, and [d] their relationship to adjacent regions indicative of permafrost-related morphologies.

Although lobate debris aprons are relatively large and have been investigated since early Viking times, some outstanding questions still remain that cover the current state of these features as well as the source of debris. Lobate debris aprons have been observed primarily along steep escarpments near the dichotomy

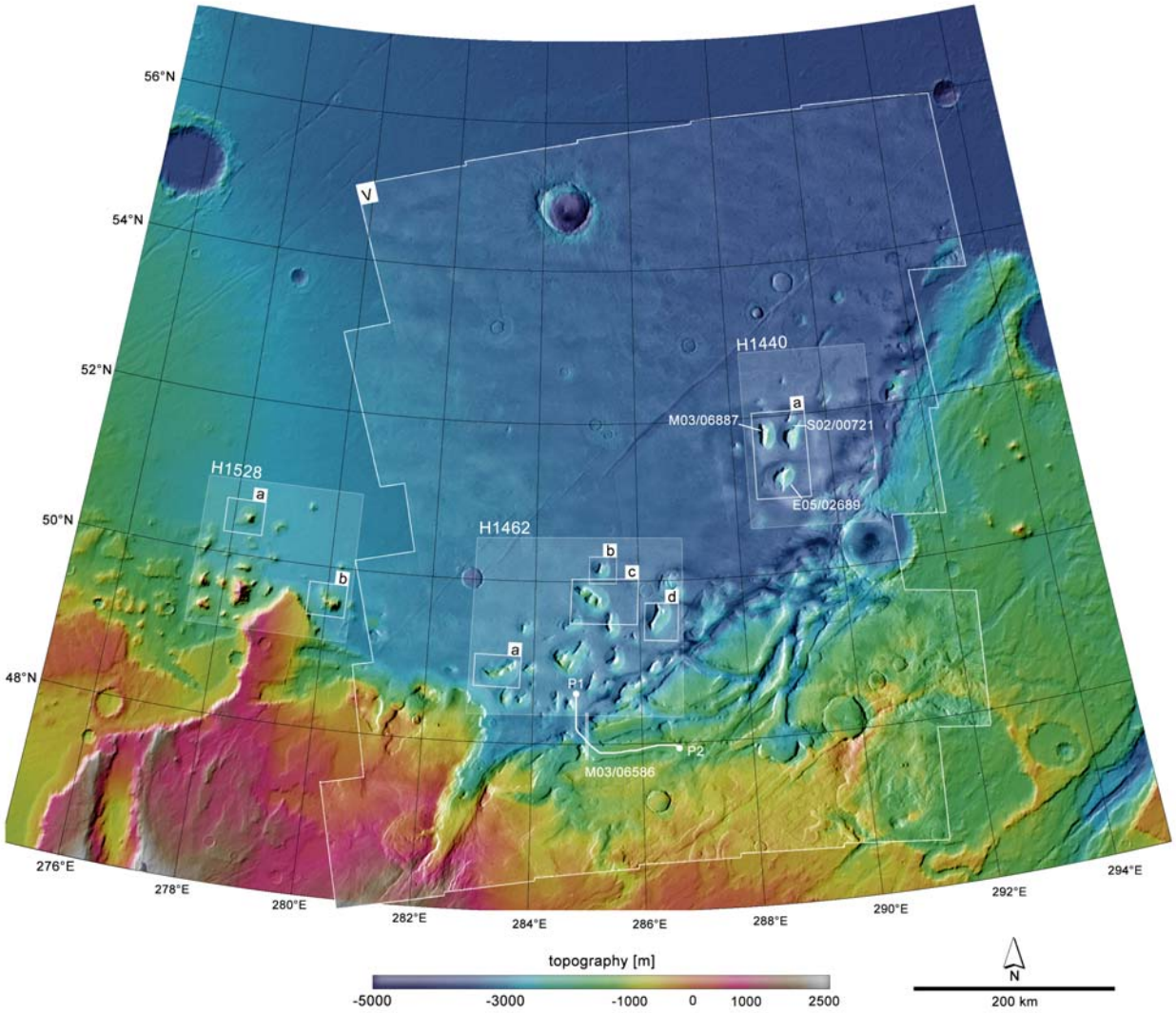

Figure 10.1.: Study area in the Tempe Terra/Mareotis Fossae region as represented by the Viking global image mosaic (MDIM-2.1) superimposed on MOLA (MEGDR) topographic data and location of image scenes discussed in the text; [V] manually processed medium-resolution Viking image mosaic composed of scenes 256S02 to 256S30 with 78-98 m/px showing more clearly albedo variations; H1528, H1462, H1440 refer to HRSC image numbers discussed in the text; lettered boxes and white outlines refer to sub-scenes depicted from HRSC image data; individual MOC scenes used in this study are labeled accordingly; P1-P2: topographic profile discussed in the text.

boundary (e.g., *Squyres*, 1978, 1979; *Mangold*, 2001) and the large impact basin of Hellas Planitia (e.g., *Squyres*, 1979; *Crown et al.*, 2002).

Rock glaciers are sensitive indicators for the climatic environment during their formation and are thought to be possible large and accessible water reservoirs (*Whalley and Azizi*, 2003).

The morphology of lobate debris aprons in Tempe Terra is similar to terrestrial talus rock glaciers (*Whalley*, 1992; *Barsch*, 1996) which are derived from footslope debris situated underneath steep wall-rock of mountainous permafrost environments.

In this study we investigate lobate debris aprons on the basis of high resolution imagery and topographic data. We first describe briefly the geologic settings and topographic/morphologic characteristics of the

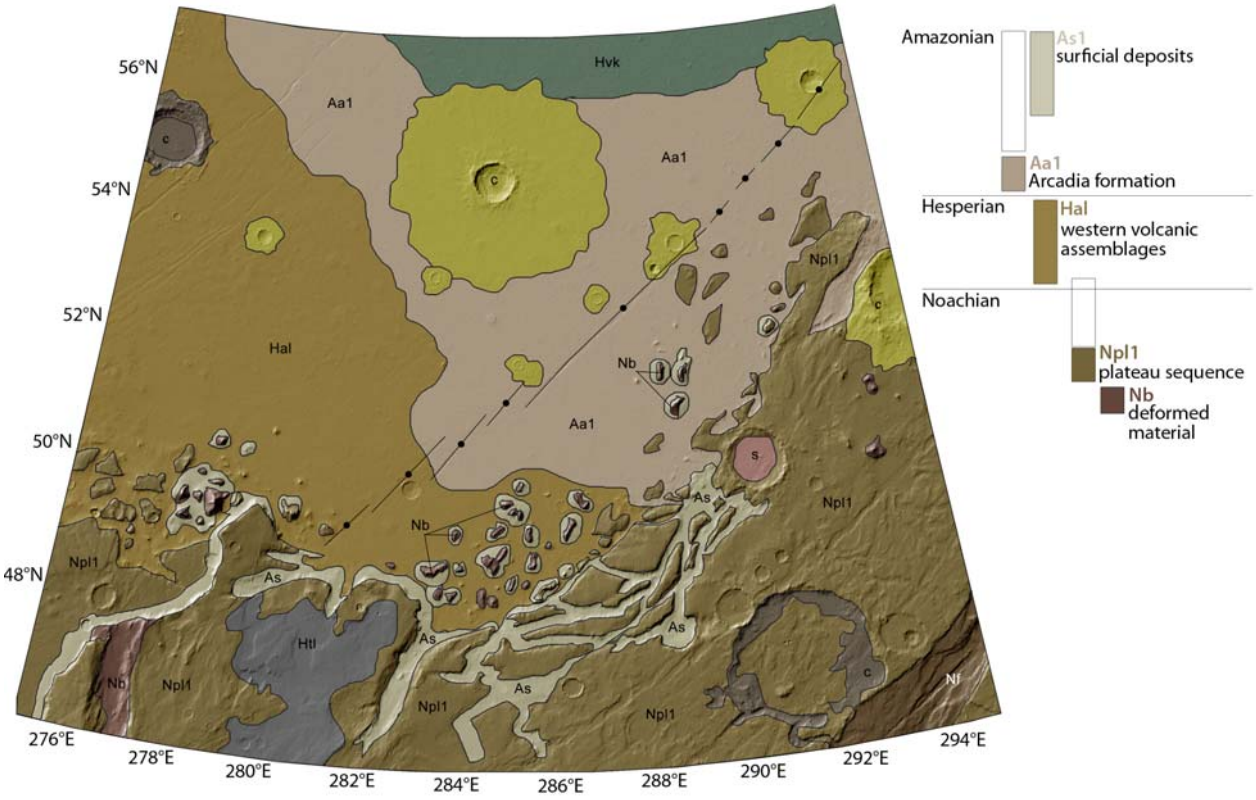

Figure 10.2.: Geologic units of the Tempe Terra area based on the geologic western hemispheric map of Mars by *Scott and Tanaka* (1986). More details regarding the distribution of Amazonian surficial deposits (unit *As*) have been added. Stratigraphic column on the right displays the most prominent units, for a complete discussion and explanation of remaining symbols see *Scott and Tanaka* (1986) and references cited therein.

study area in the northern Tempe Terra/Mareotis Fossae region (figure 10.1). In particular, we focus on an ubiquitous mantling deposit which indicates the past or present existence of near surface ice and which has contributed to debris apron formation. We then test hypotheses concerning the rheology of lobate debris aprons, analyzing their cross-sectional shape and geomorphometry.

10.2. Geologic Settings

The Tempe Terra/Mareotis Fossae region (figures 10.1 and 10.2) is located between 270°E-294°E and 46°N-54°N and is characterized by the steep dichotomy escarpment and the so-called fretted terrain (*Sharp*, 1973) which separates the study area into the southern highland assemblages and a region known as the northern lowland plains. Stratigraphically, the study area is composed of units that span Martian history from the earliest Noachian to the most recent Amazonian (figure 10.2).

We here discuss young surficial deposits interpreted as features related to creep of ice and debris (e.g., *Squyres*, 1978, 1979) and mapped as Amazonian surficial units *As* by *Scott and Tanaka* (1986) (figure 10.2). These deposits (a) fill broad fretted channels of the heavily deformed Noachian highland plateau sequence (unit *Npl1*), (b) extend from the dichotomy escarpment in northern direction, and (c) are located circumferentially to knobs and remnants of the Noachian basement unit (unit *Nb*). For reference on locations and stratigraphy see figures 10.1 and 10.2.

Remnant massifs generally form isolated knobs and hilly constructs in the northern lowlands and occur

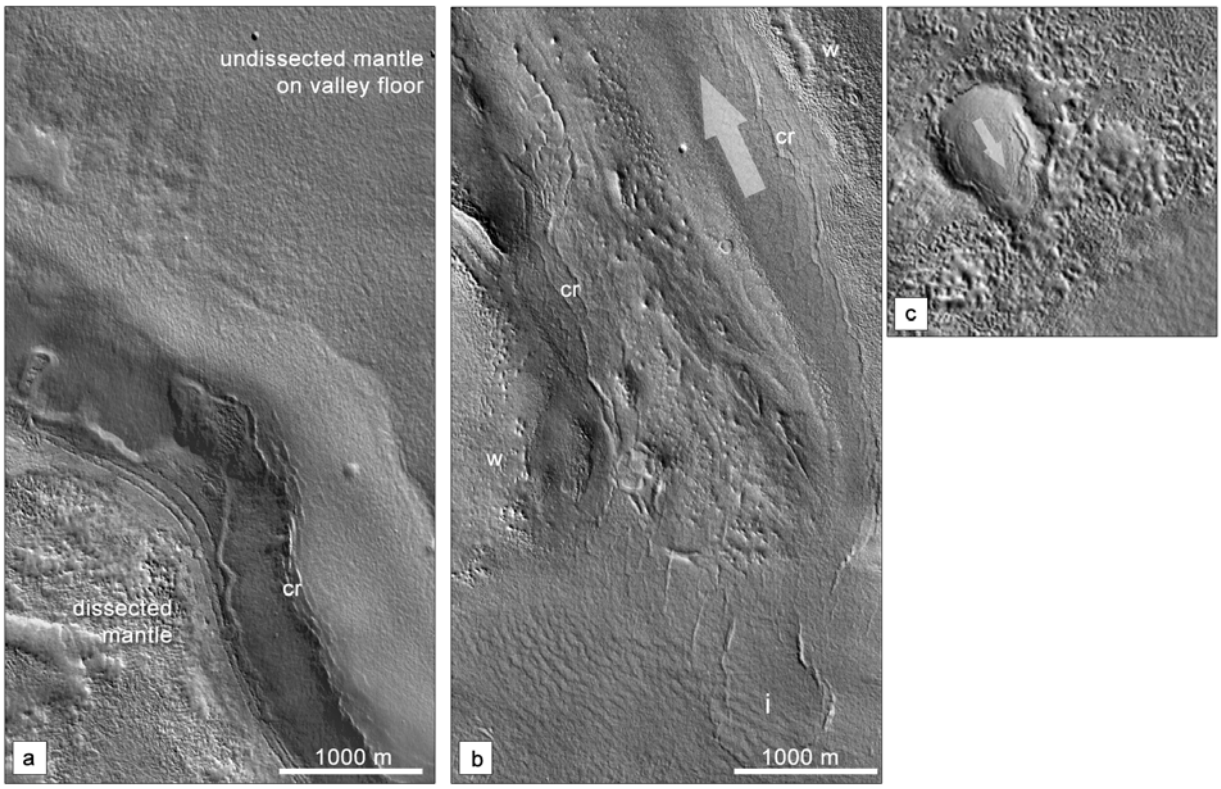

Figure 10.3.: MOC sample scenes of the dichotomy boundary (see figure 10.1 for location). [a] fretted channel floor (right) and wall (lower left). A mantling deposit is intact on the valley floor, but heavily degraded on the uplands. Crevasses (cr) on the floor of the fretted channels are characteristic of creep and flow of ice and debris. Three parallel thin ridges approximately 15-20 m wide run at constant elevations along the upper channel wall; [b] floor of a fretted channel is covered by a mantling deposit. Crevasses (cr) are situated near the channel walls (w). They also outline an impact crater completely buried by the mantle (i); [c] impact crater filled by mantling deposit. The mantle seems to have flowed out of the crater, scale is 1000 m across. Arrangements of MOC sample scenes is from south [a] to north [c], details of MOC scene M03-06586 (6.23 m/pixel), illumination is from lower left in all scenes, north is up.

more frequently close to the dichotomy escarpment and are more sparsely distributed farther to the north. In the northern lowlands, the Amazonian surficial deposits *As* cover older Hesperian units that form a lower member of the Alba Patera volcanic formation (unit *Hal*) and the lowest units of the Amazonian Arcadia formation (unit *Aa1*) of the lowlands assemblages.

Orientation of lineated valleys seems to be structurally controlled in two ways: one preferred trend is parallel to the Mareotis Fossae (50-60°NE), a system of long and narrow grabens. The other is concentric about the center of a possible impact crater in the northern lowlands (center at ~ 281°E, 56°N).

Lowland plains are characterized by wrinkle ridges and are considered to be predominantly of volcanic origin. Debris aprons at the dichotomy escarpment and remnant hills consequently are young members of the stratigraphic column; they are one of the youngest members of the Amazonian (*As*) but they are genetically related to the oldest units of the Noachian (*Nb*).

10.3. Observations

The north-south extension of the fretted terrain in our study area varies between 60 km to 170 km. The undissected upland has an elevation of -2700 m at

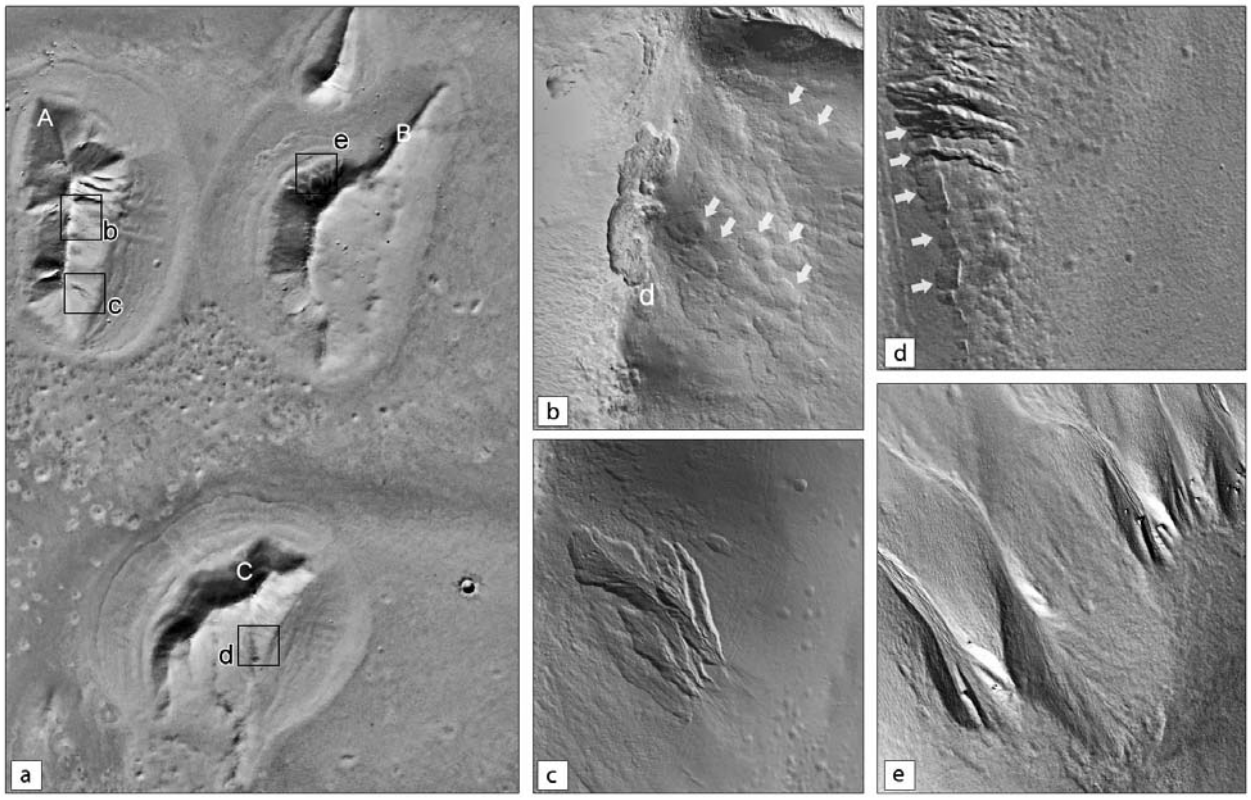

Figure 10.4.: Sample scenes of HRSC in orbit 1440 covering the easternmost study area. Labeled black boxes in [a] refer to MOC sample scenes [b-e]; see figure 10.1 for location and scales. All scenes show indications for the disintegration of a mantling deposit; [b] unusual scalloped depression at remnant crest and elliptical depressions at eastern wall (arrows); [c] overlapping gullied slide flows start at remnant wall producing faint fan deposits at terminus; [d] small slide flows incised into the footslope talus of remnant C. All incisions start at the boundary (arrows) between talus and debris apron and are located in a mantling deposit; the northernmost features are well pronounced and deeply incised while the southern features incise more surficially only; [e] slide flows incised into surficial mantling deposit of remnant B, dry masses of material accumulate as fan below terminus. Illumination is from lower left in MOC scenes [b-e], and from lower right in HRSC scene [a], north is up.

294°E and about 0 m at 280°E. The lowland has its highest elevations also in the western part of the study area (-1700 m) and slopes gently (~ 0.1°) towards NE, reaching minimum elevations of -4500 m at the eastern border of the study area. The elevation difference between uplands and lowlands decreases from ~3000 m (at 280°E) to ~1500 m (at ~274°E). This elevation difference is slightly less than that reported from the dichotomy boundary on the eastern hemisphere of Mars, i.e., Deuteronilus, Protonilus and Nilosyrtis Mensae, with 2-6 km by *Frey et al.* (1998). The highlands have a generally flat surface, sloping at an angle of less than 0.1° when measured perpendicular to the dichotomy boundary. The surfaces of very large upland segments bounded by fretted channel (figures 10.1 and 10.2) have larger slopes toward the lowlands (1°-2°) and might be tilted as blocks. Several fretted channels dissect the upland at the dichotomy boundary. Such channels have steep walls and flat floors (*Squyres*, 1978), the latter of which are often characterized by so-called "lineated valley fill" (*Squyres*, 1978, 1979), which is interpreted as material comparable to that of lobate debris aprons but confined to the valley extent. In the study area, fretted valleys have uniform

widths of ~5-10 km and constant depths of a few hundred meters.

The morphologic boundary between highland and lowland areas is characterized by two and sometimes three distinct components, (a) a steep upper slope, i.e., the wall-rock, (b) sometimes an intermediate shallow-sloped unit with downslope facing striae, and (c) the highly textured apron (*Carr*, 2001). The intermediate unit mentioned by *Carr* (2001) is only rarely observed at the isolated remnants. At a few sample locations we measured the angles of intermediate units (~6°-8°) and angles of debris aprons (~2°-4°). The results are in agreement with values presented by *Carr* (2001).

We will here focus on observations of (a) a mantling deposit and (b) the textural properties of the debris aprons, two features that can merely be separated due to their transitional nature.

1. Mantling Deposit

A mantling deposit can be observed at scarps and channels near the dichotomy boundary (figure 10.3) as well as around isolated remnant massifs and aprons (figure 10.4) that are located in the lowlands. The deposit does not show any preference to geographical or topographic location, thus, covering all parts of the study area. This observation is based on high-resolution image data (1.5-12 m/pixel) taken with the Mars Orbiter Camera (MOC) that clearly show surfaces at the dichotomy boundary that are covered by that deposit. The mantling deposit is often degraded by erosion, resulting in surfaces whose texture are highly variable, ranging from smooth over stippled, pitted, or knobby to heavily etched. In some places the mantling is completely removed. The disintegration process seems to be controlled by slope aspect (i.e., sun irradiation), the southern (sun-lit) slopes being more affected than northern slopes.

On the floors of some fretted channels we identify crevasse-like features (figure 10.3). Their specific geometry resembles that of terrestrial chevron crevasses in glaciers, which form by a combination of shear stress exerted by the valley walls and – to a minor degree – by longitudinal tensile stress (i.e., extending flow) resulting from steepening of the bed (e.g., *Benn and Evans*, 2003; *Menzies*, 2002). Lineations either parallel or perpendicular to the slopes of fretted channels and remnant massifs correspond to longitudinal or transversal lineations, respectively, and are frequently observed at terrestrial features indicative of creep of ice and debris. Such lineations can be observed at small scales as illustrated in figure 10.3. Lineations point from the interior of an impact crater towards the southern breached rim indicating direction of flow. Other lineations are formed by ridges that are thin (15-20 m wide) and extend at approximate constant elevations along upper channel walls; they seem to be genetically connected to the mantling deposit (Fig. 10.3a).

A thick mantling is also observed in a number of image scenes covering the remnant massifs of the Tempe Terra lowland: as seen in figure 10.4a, the surface of three debris aprons (A-C) appears relatively smooth although different sets of transversal ridges on the apron can still be observed. At closer inspection in MOC-scale scenes (figure 10.4b-e), the mantling texture becomes more clearly visible. The crest of remnant A is characterized by a scalloped and fretted depression (d) and sets of elliptical and aligned shallow depressions on the eastern slope which have a dimension of few tens of meters. Both, the crest depression as well as the slope depressions, are located in a mantling deposit and are indicative of material removal. Mantling-related mass-wasting features are shown in figures 10.4c-e where gullied slide flows initiate instantaneously somewhere at the mid-slope, overlap partly and produce faint terminal depositional fans (figure 10.4c-d) that are indicative of dry mass-wasting processes. As seen in figure 10.4d, the gullied slide flows can be related to a boundary where the remnant talus abuts the mantling deposit. While the northern sets of slide flows are deeply incised and well expressed, the southern are more shallow. However, not only fine-grained debris seems to be involved in the mass wasting process but also few larger blocks of material (figure 10.4e).

2. Disintegration Texture

Many debris aprons in Tempe Terra are characterized by surface textures indicative of disintegration

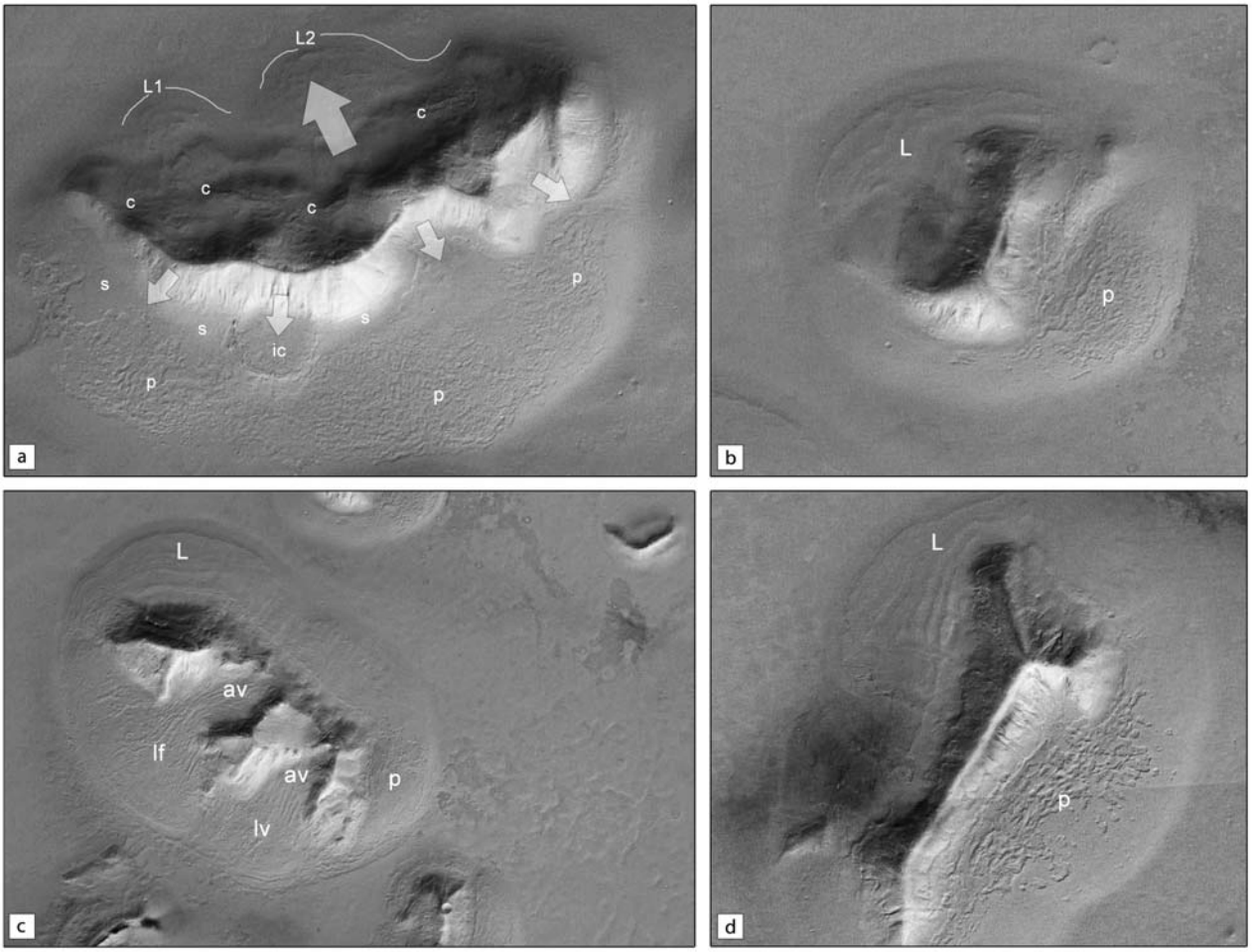

Figure 10.5.: Sample scenes of HRSC in orbit 1462 covering the central lowlands of Tempe Terra (figure 10.1); [a] arcuate remnant massif characterized by an inclined surface tilting towards North; two main directions of transport are observed: large lobes form in northern direction (L1-L2), large coherent debris masses with a pitted surface (p) advance in southern direction. An impact crater (ic) has been completely filled by erosional debris. The talus often shows areas with a smooth surface texture (s). Arcuate and sub-parallel furrows on remnant indicate extensional flow (c). [b] Small isolated remnant knob located northeast of remnant shown in [c]; northern apron texture is characterized by ridges and furrows (L), southern apron has a pitted appearance (p); [c] alcoves (av) are incised into remnant massif forming accumulation zones of debris that is subsequently transported downslope as seen in longitudinal surface lineations; [d] elongated remnant massif with well-defined crest exhibits transversal ridges and furrows (L) on northern apron and a pitted surface (p) on southern apron. Note also that all aprons are comparable in size when related to the remnant massif. For size see figure 10.1; illumination is from bottom, north is up.

of either the surficial mantling deposit or the main debris/ice body. As shown in figure 10.5a, a slightly northwards inclined and elongated remnant shows a well-pronounced debris apron emerging near the foot of the remnant. While the northern debris apron lobe is characterized by at least two large lobes with transversal ridges and overlapping lobes (L1-L2), the southern apron is more homogeneously developed with a highly pitted surface texture (p). Below the southern scarp, talus forms as expressed by a relatively smooth texture (s). Eroded remnant material has filled an old impact crater (ic). The southern scarp of the remnant is relatively steep when compared to the northern remnant slope. Flow ridges (c) indicate

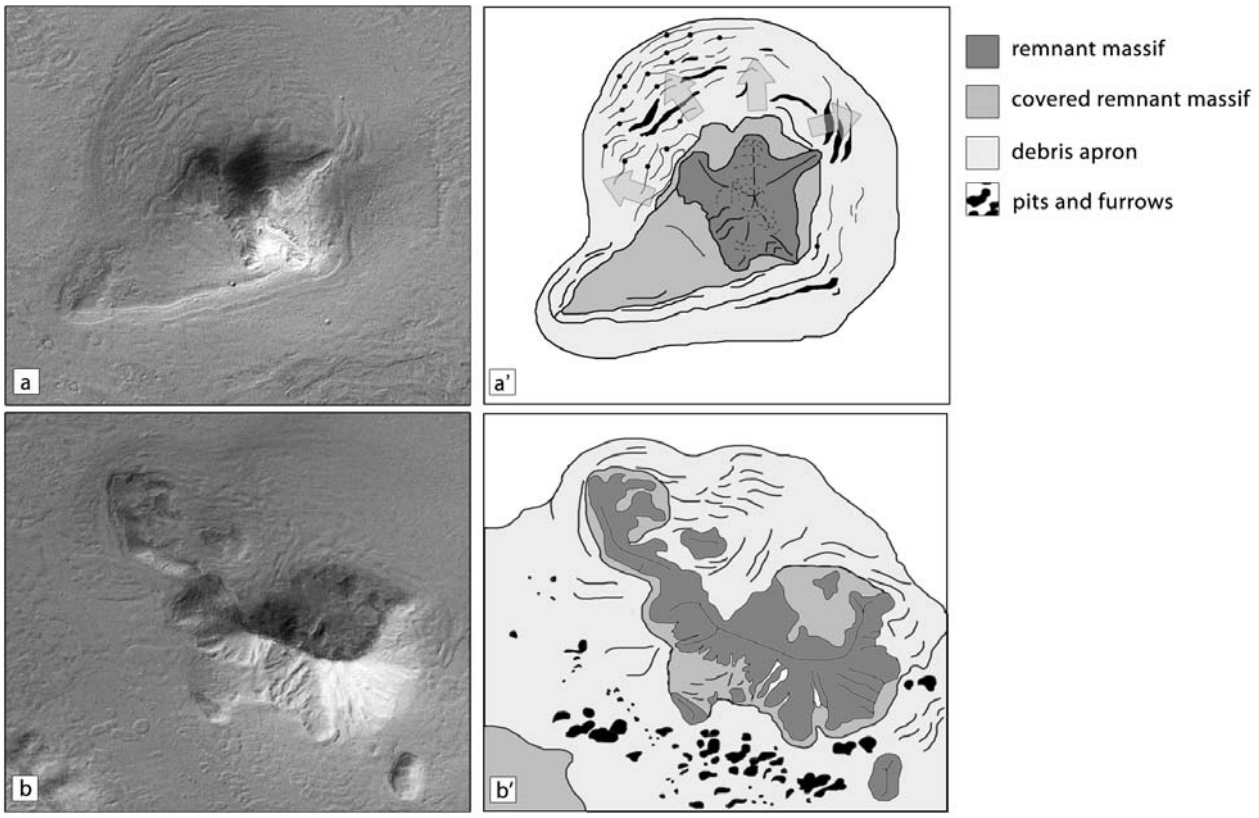

Figure 10.6.: Sample scenes of HRSC in orbit 1528 and schematic maps covering lobate debris aprons of the westernmost study area. Labeled boxes refer to labels in figure 10.1; [a-a'] isolated small remnant massif with circumferential lobate debris apron, northern apron shows pattern of ridges and valleys characteristic of compressional flow (ridges) and extensional flow (furrows); [b-b'] flow lineations at debris apron are in longitudinal configuration below alcove depression facing northeast and in transversal configuration under remnant scarp. Southern apron is characterized by pitted texture indicative of degradation. Dark gray areas represent eroded wall rock, bright gray areas are remnant surfaces that were considerably overflowed by mass wasting; irregular black spots indicate shallow depressions. For size see figure 10.1, illumination is from lower right, north is up.

that material from the remnant surface is eroding as coherent sheet masses and thus contributing to the development of the northern apron. It is noteworthy that the northern part of the remnant is heavily dissected as indicated by semi-circular scalloped depressions opening towards the north, similar to landslide scars.

Similar arrangements of transversal ridges and furrows located on a northern apron and a pitted surface texture located on the southern apron is observed in the scenes depicted in figure 10.5b,d. In figure 10.5b, the shapes of the remnant massif and debris apron are more circular and the remnant slope angles are approximately comparable in the north and south. However, the northern remnant slopes is composed of a single large bowl-shaped depression in which material is collected from the wall-rock and subsequently transported downslope towards the plains. In figure 10.5d the pitted surface in the south has not reached the terminal area of the apron but is restricted to the remnant footslope. The pitted surface (p) suggests, that this pitted surface follows a process that is gradual and initiated at the footslope.

Figure 10.5c shows well-expressed alcoves (av) at the southwestern remnant slopes and longitudinal sets of furrows and ridges (lf, lv) in the direction of maximum slope gradient. The pitted surface texture seen in figures 10.5a-b and d is here restricted to a small

area of the southeastern debris apron (p) while lobes (L) are again restricted to the northern apron.

In the westernmost region of the Tempe Terra study area, remnants and aprons are developed slightly differently when compared to those in the central and easternmost areas. Most of the remnants are characterized by a basal smooth plateau that is partly connected directly to the debris apron (figures 10.6a-a'). The northern apron slopes also show a ridge-and-furrow texture but it extends asymmetrically farther away from its source. The southern apron is more smoothly shaped. Contrasting to this, the remnant in figures 10.6b-b' is again heavily dissected by alcoves and cirque-like features. Towards the north, longitudinal and transversal ridges and furrows prevail while towards the south aprons merge with the apron of the dichotomy escarpment (lower left) and show sets of depressions at various sizes. Partly these depressions are aligned and parallel to the remnant slopes.

For few aprons measurements could be obtained to derive ages based on the crater-size frequency distribution (figure 10.7). Most of the apron surfaces show pitted and chaotic surface textures making a separation of degradational features and impact craters merely possible. Moreover, several aprons show elliptical depressions whose elongation is either perpendicular or parallel to the remnant wall. Both constellations could indicate deformation of impact craters after emplacement, one scenario being compressive, the other one being extensional.

In order to obtain the last resurfacing period only fresh-appearing craters have been mapped and clusters that were observed on the slopes of the eastern debris aprons have been excluded.

Measurements on HRSC image data provided ages in the range of 0.01 to 0.05 Ga which is consistent with data obtained from other debris apron locations on Mars (e.g., *Squyres*, 1978; *Mangold*, 2003; *Berman et al.*, 2003; *Head et al.*, 2005; *Li et al.*, 2005; *van Gasselt et al.*, 2007). For a detailed discussion on errors of age determinations see (*Neukum et al.*, 2004; *Werner*, 2005).

10.4. Geomorphometry

Lobate debris aprons were digitized using a common GIS environment in order to obtain data on areas and volumes as well as to derive shape factors describing the remnant massifs and debris aprons, such as area and volume ratios. As a basis for the digitizing process we used images of the Mars Orbiter Camera and digital elevation models from the MOLA instrument. Instead of using the gridded global MEGDR terrain models (463 m/px) we compiled the PEDR data and re-gridded it in order to get the maximum accuracy for this area, thus improving the map scale to about 350 m/px. The digitized polygons include footprint polygons delineating the basis of remnants and aprons, directions and azimuths of the longest and shortest axis of the elliptical shaped polygon, and the shortest distance from the approximate center of the mesa to the dichotomy boundary (figure 10.8).
We derived geographic coordinates, topographic elevations, lengths, areas and volumes and made simplifications with respect to the (a) base of the debris apron, which was assumed to be horizontal and flat (*Barsch*, 1996), and (b) to the volume of that part of the remnant massif located below its visible extent, i.e., covered by apron debris. We approximated that volume using the apron thickness and the area of the remnant massif. Thickness estimations, and therefore volume approximations, are based on terrain models derived from MOLA tracks and ortho-imagery. This technique was applied to all debris aprons surrounding mesas found on Mars thus far. Imprecisions are thus introduced during data gridding and the assumptions with respect to the thickness estimates. Furthermore, the terrain model data is not error-free; problems arise at several location where volume and areas are simply over- or underestimated. The accuracy of measurements depends also on the size of the object that is measured so that a trend is expected which displays overestimation of small features and probably underestimations of larger objects. In summary, errors in these measurements cannot be estimated appropriately due to too many factors that depend on a variety of factors; therefore all measure-

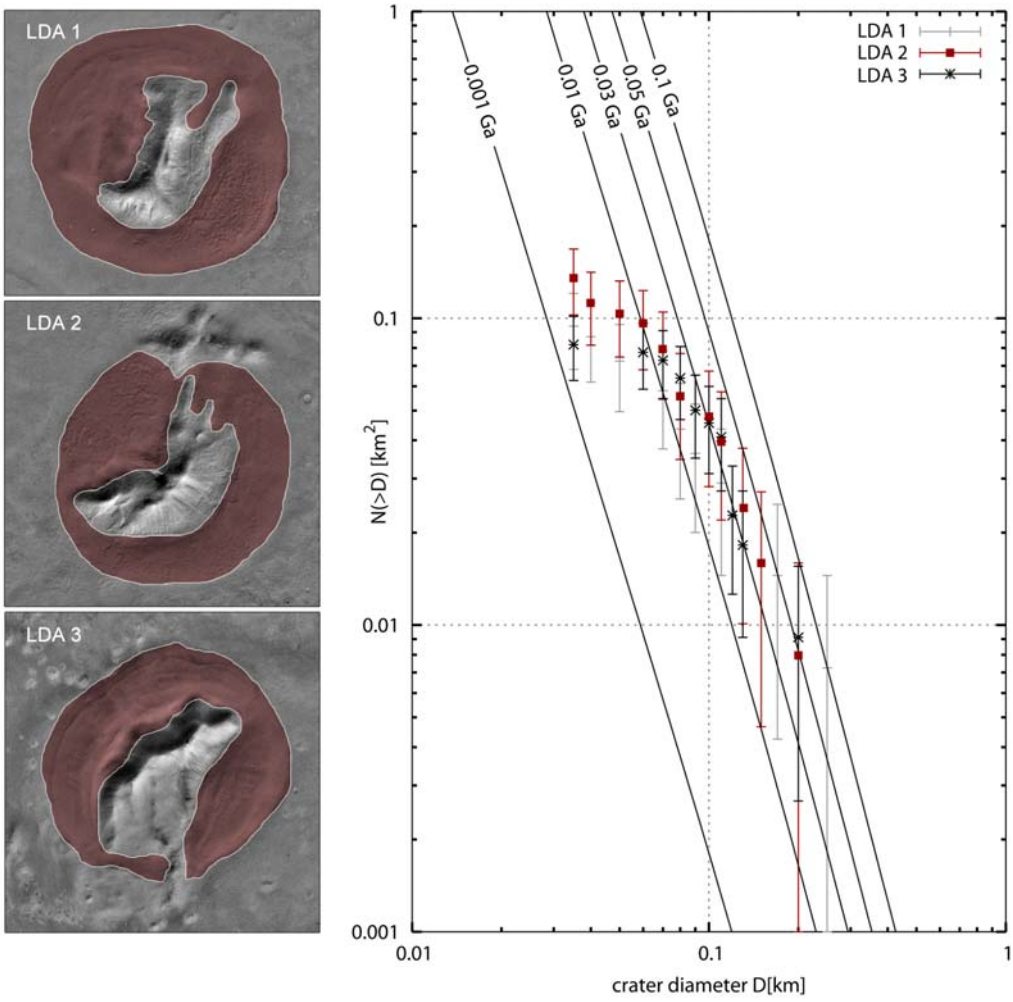

Figure 10.7.: Ages derived for debris-apron surfaces of the central and eastern part of the study area, see figure 10.1 for reference. Stair-stepped distribution indicates multiple episodes of erosional activity, derivation of isochrones (in Ga) are based on *Hartmann and Neukum* (2001) with the polynomial production function coefficients by *Ivanov* (2001); for a discussion on errors, see *Neukum et al.* (2004); *Werner* (2005).

ments are considered as trends and cannot be used to infer exact values. To avoid most of the problems, some values for volumes and areas are expressed by ratios rather than by derived absolute values.

Slope aprons in the Tempe Terra region are located between an elevation of -1700 m in the western and -3600 m in the eastern region. Mean elevations of the upper part of the apron are located at an altitude of roughly -2200 m. In plan view, the remnants north of the dichotomy boundary in Tempe Terra have a more or less irregular polygonal shape and a rugged top, in contrast to the more flat-topped mesas of the type locations in Elysium or Arabia Terra (*Mangold*, 2001). Large aprons evolve in radial direction and form an elliptical to circular-shaped footprint.

The cross-sectional shapes of the aprons are convex upward and steepening towards the terminus of the apron (figure 10.8). The length of debris aprons varies between 1.4 km to 6.3 km averaging at ~4.0 km in northern direction and ~3.5 km in southern direction. The average lengths of aprons are significantly less than values provided by *Mangold* (2001) for Deuteronilus and Protonilus Mensae with 10.8 to 33 km, and also less than those given by *Carr* (2001)

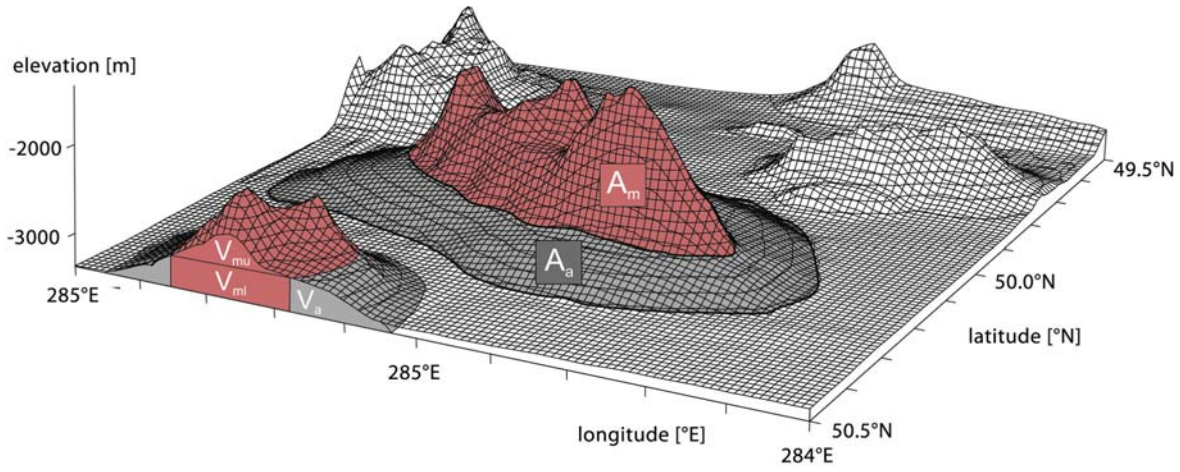

Figure 10.8.: Wiremesh-model representation of lobate debris aprons displayed in figure 10.5b and c as derived from MOLA topographic data. The small circular knob at front is truncated to show convex-upward cross-sectional shape of debris apron. Letters refer to geomorphometric values obtained in this work: A_m and $V_{mu/ml}$ are the areas and volumes, respectively, of the upper (u) as well as lower (l) remnant bodies (m); A_a and V_a refer to the area (A) and volume (V) of the debris aprons; see text for explanations on derivation of values.

and *Colaprete and Jakosky* (1998) with 15 km.

No correlation between apron or remnant length and the geographic latitude or the distance to the dichotomy boundary could be found, mostly because the Tempe Terra population of features spans a few degrees in latitude only; a correlation between direction of apron elongation and latitude could not be observed (figure 10.11).

Thicknesses of (upper) remnant massifs in Tempe Terra range from ~20 m to ~1100 m. The thickness of aprons varies between ~70 m and ~600 m under the assumption of a flat base. We observed that the relative thickness of aprons and mesas do not correlate. Furthermore, we cannot observe a correlation between the geographic latitude or distance from the boundary to the thickness of aprons and remnants. Minimum thickness values are lower than those given by *Mangold* (2001) (276 m) for the Deuteronilus area, maximum values are about the same.

Volumes of debris aprons at Tempe Terra range from <10 km³ to ~300 km³ with a mean surface area of ~282 km², ranging from ~60 km² to >1000 km² (figure 10.9). The remnants have a mean size of ~115 km² (15 to >1000 km²) and a mean volume of ~21 km³ (< 5 to 200 km³). As *Barsch* (1996) summarizes, there might be a close relationship between the source area of debris production and the surface area of a (terrestrial) rock glacier at the footslope. The ratio depends, however, on a variety of processes such as bedrock resistance, relief and climate. Several authors proposed values between 1:1.36 to 1:4.4 (*Wahrhaftig and Cox*, 1959; *Barsch*, 1977b; *Gorbunov*, 1983). Since the source area for isolated steep-walled remnants with surrounding debris aprons can be defined (i.e., the area of the remnant), we can compare the terrestrial estimates with Martian debris aprons. From the regression plot for 27 observations at Tempe Terra (Fig. 10.9) we obtain a value of $2 \cdot A_m = A_a$ [km²], with A_m being the source area and A_a the area of the debris apron. Setting the source equal to the area of the remnant massif is considered to be valid as most of the Tempe Terra remnant do not show a plateau morphology and therefore the complete surface of the remnant body provides debris for apron formation.

The volume ratio between wall rock and debris apron represents a key value for remnant degradation (figure 10.9). The volume of the visible extent of the remnant is about one-third of the volume of the apron (V_a/V_m=0.3). The measurements correlate fairly well throughout the study area and also at other locations

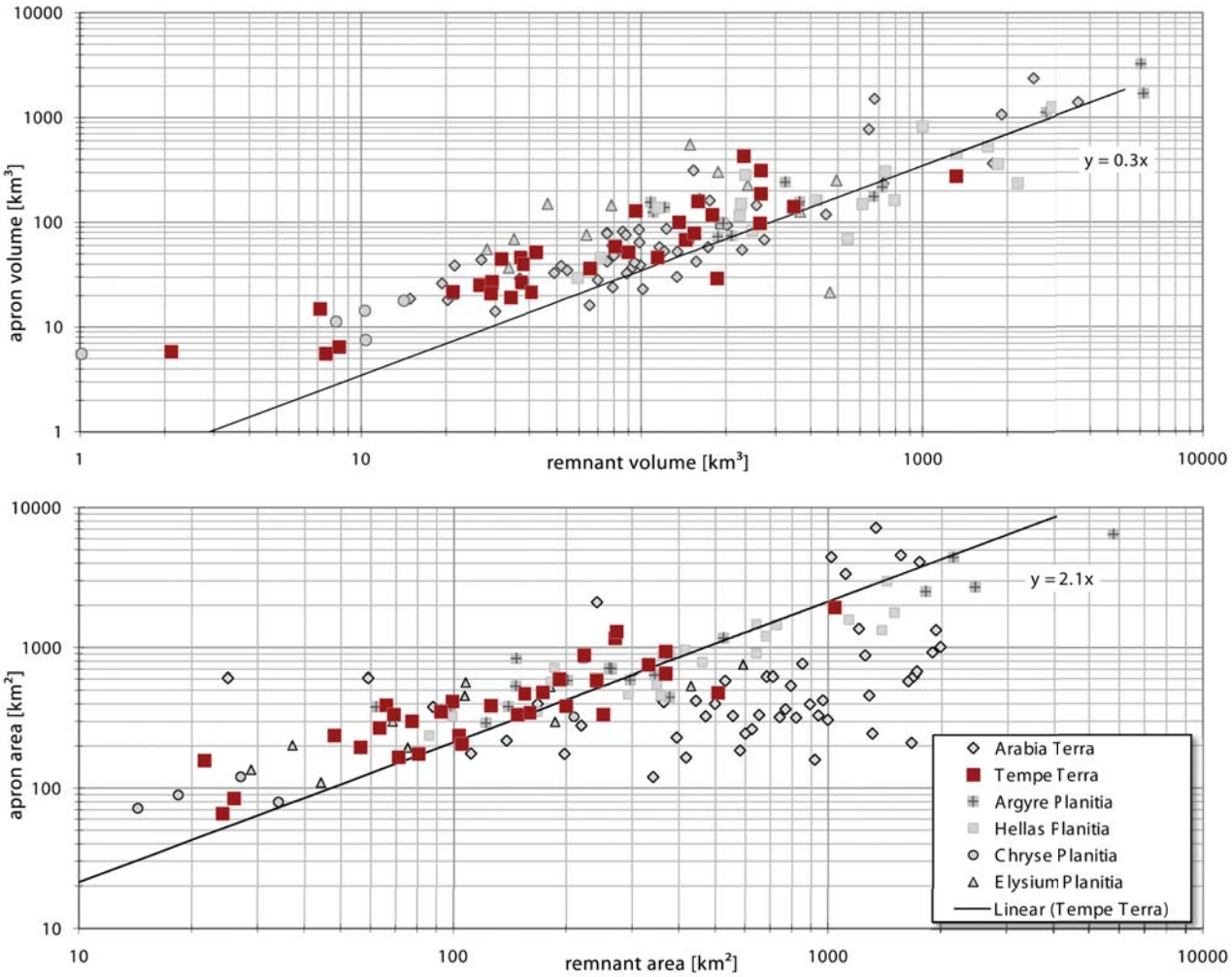

Figure 10.9.: Plot of derived ratios between volumes [a] and areas [b] of remnant massifs and debris aprons as indicator for the degradational state. Values of Tempe Terra massifs and debris aprons (dark squares) are approximated by linear fit.

on Mars (figure 10.9). According to the theory presented in *Paterson* (2001) and applied subsequently by *Squyres* (1978) and *Mangold* (2001) we used the topographic profiles to represent the theoretic shape of an ice sheet. The parabolic shape is approximated by the equation

$$(h/H)^{(2+2/n)} + (x/L)^{(1+1/n)} = 1 \qquad (10.1)$$

with h being the height at any location x, H is the overall height of the debris apron near the remnant, L is the overall length and n is a dimensionless power-law exponent used to describe flow of ice and which is between 1 and 4.2 for a glacier-flow relation and approaches ∞ under plastic deformation of ice with a yield stress of around 50-150 kPa.

Mangold (2001) calculated the basal shear stress σ (in equilibrium with yield stress) and obtained values in the range of σ =34-108 kPa for the Deuteronilus/Protonilus Mensae areas. These values are lower than photoclinometrically derived values by *Squyres* (1978). For the Tempe Terra region we obtain values between 6.7-82.4 kPa for average apron lengths, with an average of ~38 kPa using a value for the mean density of ρ = 2000 kg m^{-3} and g = 3.71 ms^{-2} for the acceleration due to gravity under Martian conditions.

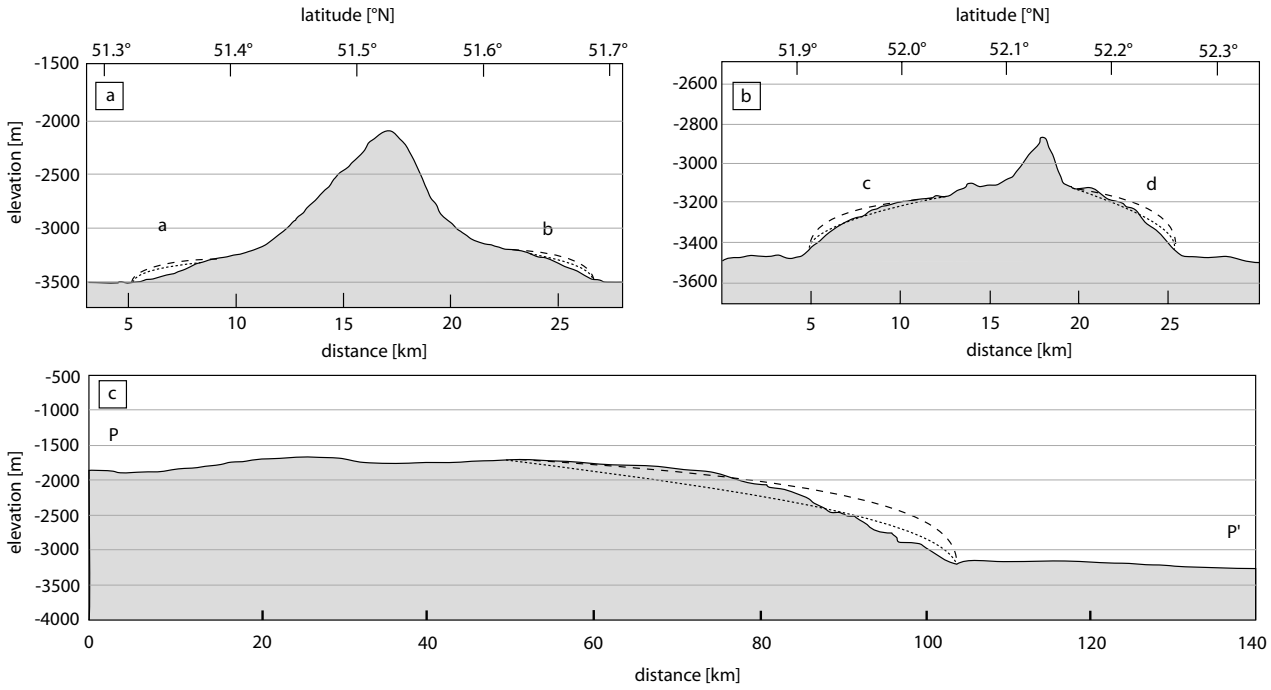

Figure 10.10.: MOLA-based topographic profiles across debris aprons [a,b] and along fretted channel [c] (see figure 10.1) and theoretic profiles of debris aprons obtained from equation derived by *Paterson* (2001). Topography of debris aprons [a, b] obtained from MOLA PEDR track 14381, profile for fretted channel obtained from gridded and interpolated PEDR track data.

Shear stresses are consistent with values given for ice sheets by *Paterson* (2001) which range from ~0 to ~100 kPa, averaging at ~50 kPa. However, the calculated values are not consistent with basal shear stresses given for terrestrial rock glaciers by *Whalley* (1992) with 100-300 kPa. This may indicate an ice content which is higher (*Hauber et al.*, 2007) than typically considered for rock glaciers or very low strain rates due to a low shear stress.

The technique of comparing theoretical topographic profiles based on the flow law relations as applied by *Squyres* (1978); *Mangold* (2001) and a variety of other authors have been tested with topographic MOLA profiles in Tempe Terra (figure 10.11). In contrast to results obtained by *Mangold* (2001) we receive unsatisfactory results when comparing both flow models.

Inactive rock glaciers tend to have generally lower slopes as either debris material was eroded or volatiles were removed, subsequently causing thermokarstic degradation of the rock-glacier surface (*Barsch*, 1996). In either case, material must have been removed in one or the other way, if the applied model is considered to be correct .

10.5. Discussion and Conclusions

Image data provides observational evidence for the existence of a wide-spread mantling deposit in the Tempe Terra/Mareotis Fossae region which covers not only debris aprons of the lowlands but also the escarpment of the Martian dichotomy boundary. At the dichotomy escarpment this mantling deposit shows several characteristics of creep and deformation as well as for processes of disintegration similar to thermokarstic degradation of ice-rich surface materials. Indicators for the mobility of that mantling deposit are found at various locations. The most prominent indicators are flow lineations in intra-crater fills and valley deposits as well as structures similar to crevasses indicative of relative movement of debris producing significant shear stresses.

Although there is evidence for fluvial sapping on the

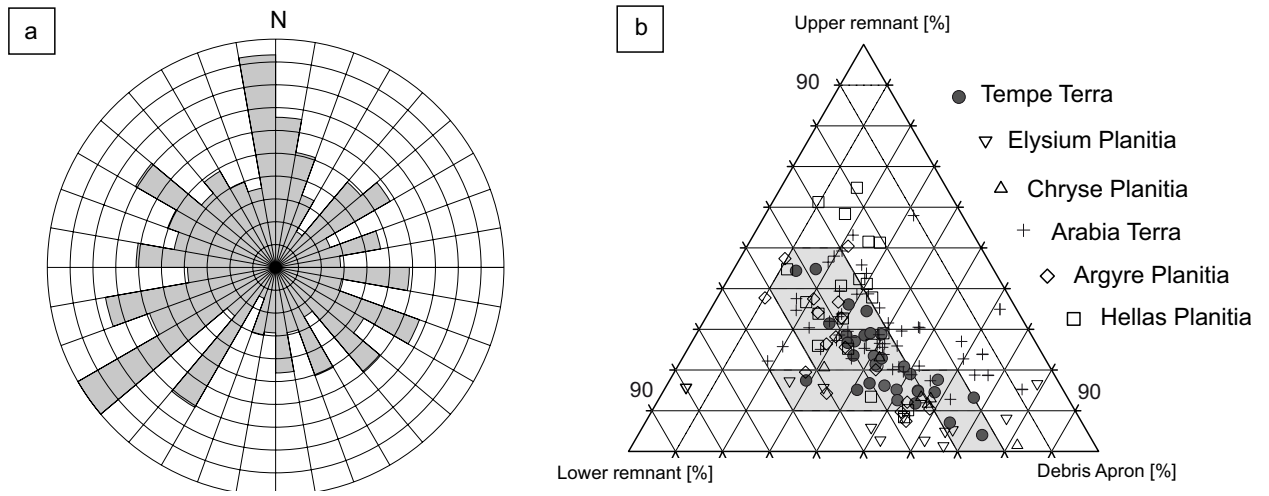

Figure 10.11.: Rose diagram of normalized mean directions of debris aprons lengths in Tempe Terra [a] and diagram showing the volume ratios of upper and lower remnant massifs and debris apron volume in comparison to ratios obtained for other debris-apron locations on Mars.

uplands near the dichotomy boundary, we find no evidence for a fluvial origin and later enlargement of fretted channels. We therefore confirm the presence of a mantle at latitudes higher than ~30-50° as inferred from global-scale roughness maps (*Kreslavsky and Head*, 2000) and directly observed in MOC images (*Carr*, 2001; *Malin and Edgett*, 2001). It was interpreted to be a mixture of ice and soil which was atmospherically deposited during a recent period of high orbital obliquity less than 100,000 a ago (*Mustard et al.*, 2001). Our investigation of MOC images confirms other observations of this deposit (*Carr*, 2001; *Mustard et al.*, 2001).

Flow lineations on debris aprons resemble closely features known from terrestrial rock glaciers comprising various sets of transversal and longitudinal ridges and furrows indicative of differential movements controlled by subsurface topography. At several locations in Tempe Terra, southward-facing debris aprons show a pitted surface texture that is interpreted as indicators for thermokarstic degeneration and loss of volatiles subsequently leading to collapse and formation of shallow depressions or pits. Their restricted extent suggest control by sun-irradiation similar to what is observed at the dichotomy escarpment (*Carr*, 2001; *Mustard et al.*, 2001). Shallow depressions form primarily in mantling material covering remnant massifs whereas pits and furrows are more often observed on the debris-apron surface. It remains unclear whether the mantling deposit or the underlying rocky debris is deformed and a clear separation of both units remains problematic to assess on the basis of image data. Numerous pristine gullied slide flows and dry mass-wasting features are commonly observed on mantling covering remnants, their limited extent suggests either local differences in the composition of the mantling material, i.e., amount of ice and debris, or structural control of the underlying topography.

Degradation of surfaces is also confirmed by observations of theoretically derived cross-profiles of debris aprons and lineated valley fill units. Both creep-related landforms show an unsatisfactory fit to the model-curve. This divergence might either be caused by limitations in the flow relation used for the model or by the eroded state of these landforms. Similar observations are known from terrestrial research and are caused by degradation of fossil or relict rock glaciers. It has been observed that topographic profiles become relatively flat or even concave (e.g., *Ikeda and Matsuoka*, 2002; *Berthling et al.*, 1998). As the results of similar comparisons in Deuteronilus and Protonilus

Mensae show a much better agreement between observations and model (*Mangold and Allemand*, 2001), we conclude that the divergence of fit is related to degradation.

The convex-upward shape of lineated valley fill at the entrance of fretted channels shows not only debris transport perpendicular to valleys walls but also in parallel direction. This furthermore indicates that flow lineations seen in lineated valley fill deposits are not only caused by compression but also by the downslope movement along the valley. Parallel thin ridges running along valley could then represent either lateral moraine-like deposits indicating former extent of lineated valley fill or they might just represent zones of higher resistance of a mantling deposit against erosion. It remains unclear which processes are responsible for the deformation of the mantling deposit. One possibility would be creep of mantling deposit, as suggested by *Milliken et al.* (2003).

Debris aprons that are found at footslopes below steep walls and large landslide scars are relatively flat and show a scalloped appearance suggestive of multiple processes that have contributed to debris supply. Smaller gullied flow features and slides covering large-scale scarps are incised into a mantling deposit. This suggests that the main processes of landsliding and rock-fall had come to an end and that subsequent deposition of a mantling deposit caused smoothing of the underlying topography and allowed formation of such slides and gullied flows.

Resurfacing ages of 0.01 to 0.05 Ga as derived on the basis of HRSC image data are consistent with ages obtained from other debris apron locations on Mars (e.g., *Squyres*, 1978; *Mangold*, 2003; *Berman et al.*, 2003; *Head et al.*, 2005; *Li et al.*, 2005; *van Gasselt et al.*, 2007) suggesting geologically recent activity.

Global geomorphometry has revealed some more details on the configuration of remnant massifs and related debris aprons and helps to put observations in Tempe Terra into a global context. Area ratios of the depositional zone and source area show values that are comparable to estimates given in *Barsch* (1996) for terrestrial rock glaciers, indicating that the genetic configuration is comparable. The fact that such area ratios compare well also for other locations on Mars suggest that debris aprons have reached an equilibrium state as suggested by e.g., *Lucchitta* (1984). The fact that debris aprons have a similar size ratio when compared to the source remnant and that they do not show obvious preferences in the direction of flow suggest that thermokarstic degradation is a process that started after debris aprons reached this equilibrium. Degradation has not yet modified aprons significantly except for some thermokarstic surficial structures which implies that this disintegration process is relatively young.

Geologically recent degradational and thermokarstic processes are in good agreement with modelling work of obliquity variations of the planet's rotational axis and variations of the planet's eccentricity and precession (e.g., *Murray et al.*, 1973; *Pollack*, 1979; *Toon et al.*, 1980; *Jakosky et al.*, 1995).

It was shown that prolonged periods of higher obliquity lead to mobilization of volatiles at the poles and to precipitation at lower latitudes (*Levrard et al.*, 2004). This process might have lead (a) to saturation of remnant-related talus deposits with ice causing subsequently creep of debris and (b) also contributed to a mid-latitudinal mantling deposit. After debris movement had reached an equilibrium state debris aprons and valley fill started to disintegrate at least surficially and in geologically recent times. □